PULL-IN ANALYSIS OF A NONLINEAR VISCOELASTIC NANOCOMPOSITE MICROPLATE UNDER AN ELECTROSTATIC ACTUATION

A. Jalali S. E. Khadem *

Department of Mechanical and Aerospace Engineering
Tarbiat Modares University
Tehran, Iran

ABSTRACT

In this paper, the deflection, natural frequency and damping quality factor of a viscoelastic microplate under an electrostatic actuation are investigated. The microplate is assumed as a CNT-reinforced nanocomposite microplate, and an electrostatic actuation is applied on it. The nonlinear equations of motion are derived using the Von-Karman plate theory, and the Kelvin-Voigt viscoelastic model. In order to obtain the material properties of the nanocomposite microplate, the Eshelby–Mori–Tanaka method is implemented. The static pull-in instability of the microplate is obtained. It is shown that the nanocomposite microplate can both increase the deflection and natural frequency of the micro devices. So, one may have a nanocomposite microplate with the same deflection of the SiO_2 microplate, while its frequency would be 1.45 times of the SiO_2 microplate. This characteristic is highly desirable in microswitches. Also, it is shown that the damping quality factor of the nanocomposite microplate is much greater than SiO_2 microplate. This fact limits the implementation of a nanocomposite microplate as a vibrating element of the micro devises. So, there are great beneficial static and frequency response characteristics for nanocomposite microplates. But, it is not recommended for microresonators due to high damping characteristics.

Keywords: Nanocomposite, Pull-in, Quality factor, Microplate.

1. INTRODUCTION

An electrically driven microplate can be implemented in various devices such as micropumps, microswitches, micromirrores and *etc*. [1-5]. Schematic of this element has been shown in Fig. 1. This element plays the role of movable electrode, and in conjunction with a fixed electrode, makes a variable capacitor. In this situation, the capacitive force causes microplate to deflect with demonstrate coupling between electrical and mechanical loading.

Such devices have been analyzed from various aspects in literatures. For example, the static deflection of a diaphragm in an electrostatic field was discussed by Francais and Dufour [6]. Dynamic characteristics of an electrostatically actuated microplate, considering geometric nonlinearities, were studied by Ng *et al*. [7]. Also, dynamic response of parallel arrays of electrostatically actuated microplates was analyzed by Porfiri [8]. All of these studies were performed using the elastic models.

Moderately large deflection with high frequency is one of the desired characteristics of a MEMS actuator/sensor. The first is the consequence of high values of wave velocity ($c = \sqrt{E/\rho}$) and the second is guaranteed due to low stiffness. As seen in Fig. 2, it is shown that among many materials that are used for micro sensors/actuators such as metals, ceramics and polymers, composite materials have the most desired properties. In this category, carbon nanotube-based composites are one of the best choices, because of exceptional mechanical properties.

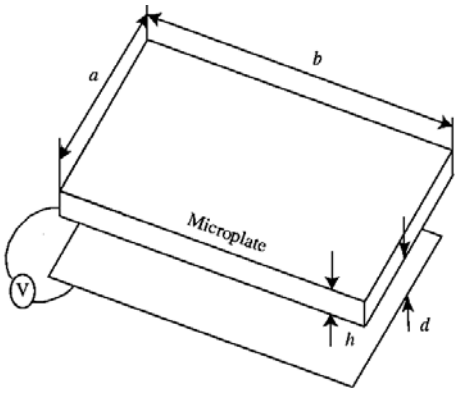


Fig. 1 Schematic of electrically driven microplate

* Corresponding author (khadem@modares.ac.ir)

DOI : 10.1017/jmech.2012.19
Copyright © 2012 The Society of Theoretical and Applied Mechanics, R.O.C.
https://doi.org/10.1017/jmech.2012.19 Published online by Cambridge University Press

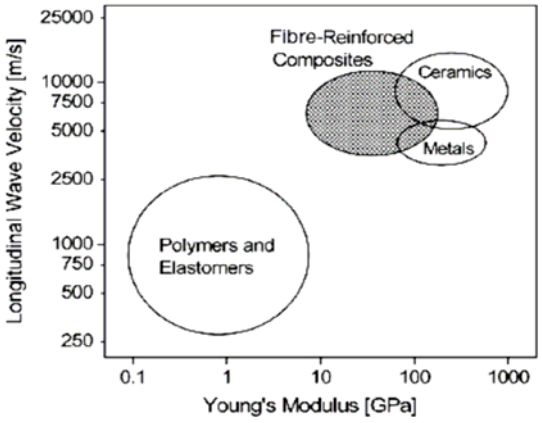


Fig. 2 Material selection charts for micro sensors/actuators [9]

CNT composite actuators/sensors have been used in recent years [10-12], and their characterization have been appeared in many new researches [13-15]. Afshari *et al*. proposed carbon nanotube reinforced composite as a new class of structural material for mechanical components of microelectomechanical systems. They investigated on the utility of CNT composites for designing actuators [9].

A CNT-reinforced composite with polymer matrix is generally assumed to be as a viscoelastic material. Fu and Zhang numerically studied nonlinear dynamic stability of an Euler-Bernouli viscoelastic microbeam under two kinds of electric forces [16]. Based on the standard linear solid model, an analysis of the nonlinear dynamic stability for a clamped-guided viscoelastic microbeam under both periodic axial force and symmetric electrostatic load were presented by Fu *et al*. In this analysis the effects of environmental and inner damping, geometric nonlinearity, creep quantity, and the symmetric electrostatic load on the principal region of instability were discussed [17].

Furthermore Fu and Zhang, in another paper, numerically studied the nonlinear static and dynamic response of a viscoelastic microplate, and discussed various forms of pull-in instability that could be appeared [18].

The response of a resonant viscoelastic microbeam to an electrostatic actuation was obtained by Zamanian *et al*. [19]. They used Galerkin method and perturbation technique to find the solution and it was shown that a small amount of viscoelastic damping could have an important effect to decrease the maximum amplitude of response and to shift the resonance frequency.

In this paper, using the Von-Karman plate theory, governing equations of motion for an immovable simply supported microplate, considering stiffness, damping and inertia nonlinearities were obtained and nonlinear response of a CNT reinforced composite microplate under electrostatic actuation was investigated. Viscoelastic behavior of the material has been modeled by Kelvin-Voigt theory. The Galerkin procedure was implemented to solve the equations of motion. The effect of CNT percentage on mechanical behavior of the microplate was studied and some useful results were obtained.

2. MODELING AND FORMULATION

Based-on Von Karmann plate theory and Kelvin-Voigt viscoelastic material modeling, the governing equations for large deflection of a rectangular viscoelastic microplate under electrostatic actuation may be obtained:

$$\begin{aligned}
&\frac{Eh}{(1-\nu^2)}\left\{\left[\frac{\partial^2 u}{\partial x^2}+\frac{\partial w}{\partial x}\frac{\partial^2 w}{\partial x^2}+\eta\left(\frac{\partial^3 u}{\partial x^2\partial t}+\frac{\partial^2 w}{\partial x\partial t}\frac{\partial^2 w}{\partial x^2}+\frac{\partial w}{\partial x}\frac{\partial^3 w}{\partial x^2\partial t}\right)\right]\right.\\
&\left.+\nu\left[\frac{\partial^2 v}{\partial x\partial y}+\frac{\partial w}{\partial y}\frac{\partial^2 w}{\partial x\partial y}+\eta\left(\frac{\partial^3 v}{\partial x\partial y\partial t}+\frac{\partial w}{\partial y}\frac{\partial^3 w}{\partial x\partial y\partial t}+\frac{\partial^2 w}{\partial y\partial t}\frac{\partial^2 w}{\partial x\partial y}\right)\right]\right\}\\
&+\frac{Eh}{2(1+\nu)}\left[\frac{\partial^2 u}{\partial y^2}+\frac{\partial^2 v}{\partial x\partial y}+\frac{\partial w}{\partial y}\frac{\partial^2 w}{\partial x\partial y}+\frac{\partial w}{\partial x}\frac{\partial^2 w}{\partial y^2}+\eta\left(\frac{\partial^3 u}{\partial y^2\partial t}+\frac{\partial^3 v}{\partial x\partial y\partial t}+\frac{\partial w}{\partial y}\frac{\partial^3 w}{\partial x\partial y\partial t}+\frac{\partial^2 w}{\partial x\partial t}\frac{\partial^2 w}{\partial y^2}\right.\right.\\
&\left.\left.+\frac{\partial^2 w}{\partial y\partial t}\frac{\partial^2 w}{\partial x\partial y}+\frac{\partial w}{\partial x}\frac{\partial^3 w}{\partial y^2\partial t}\right)\right]=\rho h\frac{\partial^2 u}{\partial t^2}
\end{aligned}\tag{1}$$

$$\begin{aligned}
&\frac{Eh}{(1-\nu^2)}\left\{\left[\frac{\partial^2 v}{\partial y^2}+\frac{\partial w}{\partial y}\frac{\partial^2 w}{\partial y^2}+\eta\left(\frac{\partial^3 v}{\partial y^2\partial t}+\frac{\partial^2 w}{\partial y\partial t}\frac{\partial^2 w}{\partial y^2}+\frac{\partial w}{\partial y}\frac{\partial^3 w}{\partial y^2\partial t}\right)\right]\right.\\
&\left.+\nu\left[\frac{\partial^2 u}{\partial x\partial y}+\frac{\partial w}{\partial x}\frac{\partial^2 w}{\partial x\partial y}+\eta\left(\frac{\partial^3 u}{\partial x\partial y\partial t}+\frac{\partial w}{\partial x}\frac{\partial^3 w}{\partial x\partial y\partial t}+\frac{\partial^2 w}{\partial x\partial t}\frac{\partial^2 w}{\partial x\partial y}\right)\right]\right\}\\
&+\frac{Eh}{2(1+\nu)}\left[\frac{\partial^2 u}{\partial x\partial y}+\frac{\partial^2 v}{\partial x^2}+\frac{\partial w}{\partial y}\frac{\partial^2 w}{\partial x^2}+\frac{\partial w}{\partial x}\frac{\partial^2 w}{\partial x\partial y}+\eta\left(\frac{\partial^3 u}{\partial x\partial y\partial t}+\frac{\partial^3 v}{\partial x^2\partial t}+\frac{\partial w}{\partial y}\frac{\partial^3 w}{\partial x^2\partial t}+\frac{\partial^2 w}{\partial y\partial t}\frac{\partial^2 w}{\partial x^2}\right.\right.\\
&\left.\left.+\frac{\partial^2 w}{\partial x\partial t}\frac{\partial^2 w}{\partial x\partial y}+\frac{\partial w}{\partial x}\frac{\partial^3 w}{\partial x\partial y\partial t}\right)\right]=\rho h\frac{\partial^2 v}{\partial t^2}
\end{aligned}\tag{2}$$

https://doi.org/10.1017/jmech.2012.19 Published online by Cambridge University Press

$$-\frac{1}{12}h^2\left(\frac{\partial^4 w}{\partial x^4}+2\frac{\partial^4 w}{\partial x^2\partial y^2}+\frac{\partial^4 w}{\partial y^4}\right)-\frac{1}{12}h^2\eta\left(\frac{\partial^5 w}{\partial x^4\partial t}+2\frac{\partial^5 w}{\partial x^2\partial y^2\partial t}+\frac{\partial^5 w}{\partial y^4\partial t}\right)$$
$$+\left[\frac{\partial u}{\partial x}+\nu\frac{\partial v}{\partial y}+\frac{1}{2}\left(\left(\frac{\partial w}{\partial x}\right)^2+\nu\left(\frac{\partial w}{\partial y}\right)^2\right)+\frac{(1-\nu^2)N_{xx}}{Eh}+\eta\left(\frac{\partial^2 u}{\partial x\partial t}+\nu\frac{\partial^2 v}{\partial y\partial t}+\frac{\partial w}{\partial x}\frac{\partial^2 w}{\partial x\partial t}+\nu\frac{\partial w}{\partial y}\frac{\partial^2 w}{\partial y\partial t}\right)\right]\frac{\partial^2 w}{\partial x^2}$$
$$+\left[\frac{\partial v}{\partial y}+\nu\frac{\partial u}{\partial x}+\frac{1}{2}\left(\left(\frac{\partial w}{\partial y}\right)^2+\nu\left(\frac{\partial w}{\partial x}\right)^2\right)+\frac{(1-\nu^2)N_{yy}}{Eh}+\eta\left(\frac{\partial^2 v}{\partial y\partial t}+\nu\frac{\partial^2 u}{\partial x\partial t}+\nu\frac{\partial w}{\partial x}\frac{\partial^2 w}{\partial x\partial t}+\frac{\partial w}{\partial y}\frac{\partial^2 w}{\partial y\partial t}\right)\right]\frac{\partial^2 w}{\partial y^2}$$
$$+(1-\nu)\left[\frac{\partial u}{\partial y}+\frac{\partial v}{\partial x}+\frac{\partial w}{\partial x}\frac{\partial w}{\partial y}+2\frac{(1+\nu)N_{xy}}{Eh}+\eta\left(\frac{\partial^2 u}{\partial y\partial t}+\frac{\partial^2 v}{\partial x\partial t}+\frac{\partial^2 w}{\partial x\partial t}\frac{\partial w}{\partial y}+\frac{\partial w}{\partial x}\frac{\partial^2 w}{\partial y\partial t}\right)\right]\frac{\partial^2 w}{\partial x\partial y}$$
$$=C_p^{-2}\left(\frac{\partial^2 w}{\partial t^2}-\rho h\frac{\partial^2 u}{\partial t^2}\frac{\partial w}{\partial x}-\rho h\frac{\partial^2 v}{\partial t^2}\frac{\partial w}{\partial y}\right)-\frac{\varepsilon_0(1-\nu^2)*(V_p+V_d)^2}{2Ehd^2\left(1-\frac{w}{d}\right)^2} \tag{3}$$

and the boundary conditions for an immovable simply supported microplate are:

$$\begin{aligned} &x=0,a \quad , \quad u=v=w=0 \quad , \quad \text{and} \quad \frac{\partial^2 w}{\partial x^2}=0 \\ &y=0,b \quad , \quad u=v=w=0 \quad , \quad \text{and} \quad \frac{\partial^2 w}{\partial y^2}=0 \end{aligned} \tag{4}$$

in which $u = u(x, y, t)$, $v = v(x, y, t)$ and $w = w(x, y, t)$ are the displacements of microplate in X, Y and Z directions, η is the Kelvin-Voigt viscoelastic damping coefficient which is defined by $\eta = C/E$, where C is the viscoelastic damping of the material, E is the Young's modulus, ν is the Poisson' ratio, h is the plate thickness, ρ is the material density, d is the air gap, ε_0 is the dielectric constant, and V_p and V_d are the polarization and fluctuation component of the applied voltage. The Eqs. (1) ~ (3) can be presented in non-dimensional form using the following non-dimensional parameters:

$$\begin{aligned} &x^*=\frac{x}{a}\,,\ y^*=\frac{y}{b}\,,\ t^*=\frac{t}{\tau}\,,\ u^*=\frac{au}{d^2}\,,\ v^*=\frac{av}{d^2}\,, \\ &w^*=\frac{w}{d},\ \eta^*=\frac{\eta}{\tau} \end{aligned} \tag{5}$$

in which $\tau=\sqrt{12}a^2/hc_p$, and $c_p^2=E/\rho(1-\nu^2)$. So, substituting Eq. (5) into Eqs. (1) ~ (3), and dropping " * " from the variables, the non-dimensional form of Eqs. (1) ~ (3) would be:

$$\frac{\partial^2 u}{\partial x^2}+\frac{\partial w}{\partial x}\frac{\partial^2 w}{\partial x^2}+\eta\left(\frac{\partial^3 u}{\partial x^2\partial t}+\frac{\partial^2 w}{\partial x\partial t}\frac{\partial^2 w}{\partial x^2}+\frac{\partial w}{\partial x}\frac{\partial^3 w}{\partial x^2\partial t}\right)$$
$$+\nu\left[c\frac{\partial^2 v}{\partial x\partial y}+c^2\frac{\partial w}{\partial y}\frac{\partial^2 w}{\partial x\partial y}+\eta\left(c\frac{\partial^3 v}{\partial x\partial y\partial t}+c^2\frac{\partial w}{\partial y}\frac{\partial^3 w}{\partial x\partial y\partial t}+c^2\frac{\partial^2 w}{\partial y\partial t}\frac{\partial^2 w}{\partial x\partial y}\right)\right]$$
$$+\frac{(1-\nu)}{2}\left[c^2\frac{\partial^2 u}{\partial y^2}+c\frac{\partial^2 v}{\partial x\partial y}+c^2\frac{\partial w}{\partial y}\frac{\partial^2 w}{\partial x\partial y}+c^2\frac{\partial w}{\partial x}\frac{\partial^2 w}{\partial y^2}+\eta\left(c^2\frac{\partial^3 u}{\partial y^2\partial t}+c\frac{\partial^3 v}{\partial x\partial y\partial t}+c^2\frac{\partial w}{\partial y}\frac{\partial^3 w}{\partial x\partial y\partial t}\right.\right.$$
$$\left.\left.+c^2\frac{\partial^2 w}{\partial x\partial t}\frac{\partial^2 w}{\partial y^2}+c^2\frac{\partial^2 w}{\partial y\partial t}\frac{\partial^2 w}{\partial x\partial y}+c^2\frac{\partial w}{\partial x}\frac{\partial^3 w}{\partial y^2\partial t}\right)\right]=\frac{h^2}{12a^2}\frac{\partial^2 u}{\partial t^2} \tag{6}$$

$$c^2\frac{\partial^2 v}{\partial y^2}+c^3\frac{\partial w}{\partial y}\frac{\partial^2 w}{\partial y^2}+\eta\left(c^2\frac{\partial^3 v}{\partial y^2\partial t}+c^3\frac{\partial^2 w}{\partial y\partial t}\frac{\partial^2 w}{\partial y^2}+c^3\frac{\partial w}{\partial y}\frac{\partial^3 w}{\partial y^2\partial t}\right)+\nu\left[c\frac{\partial^2 u}{\partial x\partial y}+c\frac{\partial w}{\partial x}\frac{\partial^2 w}{\partial x\partial y}+\right.$$
$$\left.\eta\left(c\frac{\partial^3 u}{\partial x\partial y\partial t}+c\frac{\partial w}{\partial x}\frac{\partial^3 w}{\partial x\partial y\partial t}+c\frac{\partial^2 w}{\partial x\partial t}\frac{\partial^2 w}{\partial x\partial y}\right)\right]$$
$$+\frac{(1-\nu)}{2}\left[c\frac{\partial^2 u}{\partial x\partial y}+\frac{\partial^2 v}{\partial x^2}+c\frac{\partial w}{\partial y}\frac{\partial^2 w}{\partial x^2}+c\frac{\partial w}{\partial x}\frac{\partial^2 w}{\partial x\partial y}+\eta\left(c\frac{\partial^3 u}{\partial x\partial y\partial t}+\frac{\partial^3 v}{\partial x^2\partial t}+c\frac{\partial w}{\partial y}\frac{\partial^3 w}{\partial x^2\partial t}+c\frac{\partial^2 w}{\partial y\partial t}\frac{\partial^2 w}{\partial x^2}+\right.\right.$$
$$\left.\left.c\frac{\partial^2 w}{\partial x\partial t}\frac{\partial^2 w}{\partial x\partial y}+c\frac{\partial w}{\partial x}\frac{\partial^3 w}{\partial x\partial y\partial t}\right)\right]=\frac{h^2}{12a^2}\frac{\partial^2 v}{\partial t^2} \tag{7}$$

https://doi.org/10.1017/jmech.2012.19 Published online by Cambridge University Press

$$-\left(\frac{\partial^4 w}{\partial x^4}+2\frac{\partial^4 w}{\partial x^2\partial y^2}+\frac{\partial^4 w}{\partial y^4}\right)-\eta\left(\frac{\partial^5 w}{\partial x^4\partial t}+2\frac{\partial^5 w}{\partial x^2\partial y^2\partial t}+\frac{\partial^5 w}{\partial y^4\partial t}\right)$$

$$+12\alpha_1\left[\frac{\partial u}{\partial x}+\nu c\frac{\partial v}{\partial y}+\frac{1}{2}\left(\left(\frac{\partial w}{\partial x}\right)^2+\nu c^2\left(\frac{\partial w}{\partial y}\right)^2\right)+N_1+\eta\left(\frac{\partial^2 u}{\partial x\partial t}+\nu c\frac{\partial^2 v}{\partial y\partial t}+\frac{\partial w}{\partial x}\frac{\partial^2 w}{\partial x\partial t}+\nu c^2\frac{\partial w}{\partial y}\frac{\partial^2 w}{\partial y\partial t}\right)\right]\frac{\partial^2 w}{\partial x^2}$$

$$+12c^2\alpha_1\left[c\frac{\partial v}{\partial y}+\nu\frac{\partial u}{\partial x}+\frac{1}{2}\left(c^2\left(\frac{\partial w}{\partial y}\right)^2+\nu\left(\frac{\partial w}{\partial x}\right)^2\right)+N_2+\eta\left(c\frac{\partial^2 v}{\partial y\partial t}+\nu\frac{\partial^2 u}{\partial x\partial t}+\nu\frac{\partial w}{\partial x}\frac{\partial^2 w}{\partial x\partial t}+c^2\frac{\partial w}{\partial y}\frac{\partial^2 w}{\partial y\partial t}\right)\right]\frac{\partial^2 w}{\partial y^2}$$

$$+12c(1-\nu)\alpha_1\left[c\frac{\partial u}{\partial y}+\frac{\partial v}{\partial x}+c\frac{\partial w}{\partial x}\frac{\partial w}{\partial y}+N_{12}+\eta\left(c\frac{\partial^2 u}{\partial y\partial t}+\frac{\partial^2 v}{\partial x\partial t}+c\frac{\partial^2 w}{\partial x\partial t}\frac{\partial w}{\partial y}+c\frac{\partial w}{\partial x}\frac{\partial^2 w}{\partial y\partial t}\right)\right]\frac{\partial^2 w}{\partial x\partial y}$$

$$=\frac{\partial^2 w}{\partial t^2}-\frac{\partial w}{\partial x}\frac{\partial^2 u}{\partial t^2}-\frac{\partial w}{\partial y}\frac{\partial^2 v}{\partial t^2}-\alpha_2\frac{(V_p+V_i)^2}{(1-w)^2} \tag{8}$$

and the non-dimensional boundary conditions are:

$$\begin{aligned} &x=0,1\,,\quad u=v=w=0\,,\quad \text{and}\quad \frac{\partial^2 w}{\partial x^2}=0\\ &y=0,1\,,\quad u=v=w=0\,,\quad \text{and}\quad \frac{\partial^2 w}{\partial y^2}=0 \end{aligned} \tag{9}$$

As seen in these equations the stiffness, damping and inertia nonlinearities were included. The parameters appeared in these equations are:

$$c=\frac{a}{b}\,,\ \alpha_1=\frac{d^2}{h^2}\,,\ \alpha_2=\frac{6\varepsilon_0(1-\nu^2)a^4}{E\,h^3\,d^3} \tag{10}$$

3. PROPERTIES ESTIMATION OF NANOCOMPOSITES

Carbon nanotubes are the most remarkable materials discovered by Iijima [20]. There are two common types of nanotubes, namely single-walled carbon nanotube (SWNT) and multi-wall carbon nanotube (MWNT). Nominal properties of these materials have been listed in Table 1.

In this paper, a (10, 10) SWNT was selected as a reinforcement and Polymethyl methacrylate (PMMA) as a matrix material because of its good variable-climate-resisting property.

Table 2 has listed the material characteristics for typical material, used in this study. SiO_2 is one of the traditional materials used as a basic element of the micro devices that behaves as an elastic material and PMMA has been selected as a matrix element of viscoelastic nanocomposite material.

The elastic modulus of CNT/PMMA nanocomposite was estimated by Eshelby–Mori–Tanaka method [21]. An essential ingredient of the Eshelby–Mori–Tanaka method is the approximation of short fibers as ellipsoidal inclusions of aspect ratio $s = L/2r$. So, the Young's modulus of the nanocomposite is obtained as:

$$C^C = C^M + V_f\left\langle (C^N - C^M)A^N\right\rangle\left[(1-V_f)I + V_f < A^N >\right]^{-1} \tag{11}$$

in which C^C, C^M and C^N are stiffness tensors of composite, matrix and nano fiber, respectively, I is the identity tensor and A^N is defined as:

Table 1 Properties of nanotubes

	(10,10) SWNTs	$(30,30)_{10}$ MWNTs	Array of (10,10) SWNTs
E_{11} (GPa)	1060	800	580
E_{22} (GPa)	6.63	15.58	9.4
ν	0.16	0.14	0.18
ρ (Kg/m^3)	1440	2090	1150

Table 2 Properties of bulk materials

Material	ρ (Kg/m^3)	E_{11}(GPa)	ν
SiO_2	2600	70	0.2
PMMA	1150	3	0.4

$$A^N = \left[I + S(C^M)^{-1}(C^N - C^M)\right]^{-1} \tag{12}$$

where S is the Eshelby tensor. The elements of the Eshelby tensor are functions of the aspect ratio of the inclusion, s, and the Poisson's ratio of the matrix. These elements are defined in Table 3

in which:

$$I_1 = \frac{2s}{\sqrt{(1-s^2)^3}}\left[s\sqrt{s^2-1} - \cosh^{-1}(s)\right] \tag{13}$$

https://doi.org/10.1017/jmech.2012.19 Published online by Cambridge University Press

Table 3 elements of Eshelby tensor [21]

	Ellipsoid (aspect ratio, s)
S_{11}	$4Q/3 + RI_3 + 2s^2T$
$S_{22} = S_{33}$	$Q + RI_1 + 3T/4$
$S_{23} = S_{32}$	$Q/3 - RI_1 + 4T/3$
$S_{21} = S_{31}$	$-RI_1 - s^2T$
$S_{12} = S_{13}$	$-RI_3 - T$
S_{44}	$Q/3 + RI_1 + T/4$
$S_{55} = S_{66}$	$2R - RI_1 / 2 - 1 + s^2 / 2 \cdot T$
For other S_{ij}	0

$$Q = \frac{3}{8(1-\nu^M)}, \quad R = \frac{1-2\nu^M}{8(1-\nu^M)},$$
$$T = Q\frac{4-3I_1}{3(s^2-1)}, \quad I_3 = 4-2I_1 \tag{14}$$

Considering a random orientation distribution of fibers, and the aspect ratio of fibers greater than 1000, the elastic modulus of SWNT/PMMA nanocomposite with respect to volume fraction of CNT has been shown in Fig. 3. As shown in this figure, for 32.2% volume fraction of SWNT, the elastic modulus of nanocomposite would be equal to SiO_2 one.

4. STATIC RESPONSE OF THE MICROPLATE

The microplate deflections under electrostatic force are composed of a static component due to a DC voltage and a fluctuation component due to the AC voltage. So, one can rewrite the plate deflections in the form of:

$$u(x, y, t) = u_s(x, y) + u_d(x, y, t)$$
$$v(x, y, t) = v_s(x, y) + u_d(x, y, t)$$
$$w(x, y, t) = w_s(x, y) + w_d(x, y, t) \tag{15}$$

In these equations, subscript " s " and " d " denotes static and fluctuating component of deflections. Substituting Eq. (15) into Eqs. (6) ~ (8), the governing equations of dynamic response of the microplate about deflected position are obtained.

In order to extract equations of static response of the microplate, terms with time derivatives have been assumed to be zero. So the static response equations would be:

$$\frac{\partial^2 u_s}{\partial x^2} + \frac{\partial w_s}{\partial x}\frac{\partial^2 w_s}{\partial x^2} + \nu\left(c\frac{\partial^2 v_s}{\partial x \partial y} + c^2\frac{\partial w_s}{\partial y}\frac{\partial^2 w_s}{\partial x \partial y}\right)$$
$$+\frac{(1-\nu)}{2}\left[c^2\frac{\partial^2 u_s}{\partial y^2} + c\frac{\partial^2 v_s}{\partial x \partial y} + c^2\frac{\partial w_s}{\partial y}\frac{\partial^2 w_s}{\partial x \partial y} + c^2\frac{\partial w_s}{\partial x}\frac{\partial^2 w_s}{\partial y^2}\right] = 0 \tag{16}$$

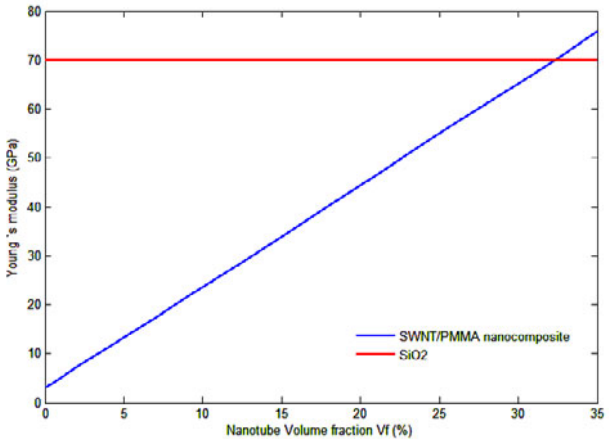


Fig. 3 Young's modulus of fully random dispersed SWNT/PMMA nano composite

$$c^2\frac{\partial^2 v_s}{\partial y^2} + c^3\frac{\partial w_s}{\partial y}\frac{\partial^2 w_s}{\partial y^2} + \nu\left(c\frac{\partial^2 u_s}{\partial x \partial y} + c\frac{\partial w_s}{\partial x}\frac{\partial^2 w_s}{\partial x \partial y}\right)$$
$$+\frac{(1-\nu)}{2}\left[c\frac{\partial^2 u_s}{\partial x \partial y} + \frac{\partial^2 v_s}{\partial x^2} + c\frac{\partial w_s}{\partial y}\frac{\partial^2 w_s}{\partial x^2} + c\frac{\partial w_s}{\partial x}\frac{\partial^2 w_s}{\partial x \partial y}\right] = 0 \tag{17}$$

$$-\left(\frac{\partial^4 w_s}{\partial x^4} + 2c^2\frac{\partial^4 w_s}{\partial x^2 \partial y^2} + c^4\frac{\partial^4 w_s}{\partial y^4}\right)$$
$$+12\alpha_1\left[\frac{\partial u_s}{\partial x} + \nu c\frac{\partial v_s}{\partial y} + \frac{1}{2}\left(\left(\frac{\partial w_s}{\partial x}\right)^2 + \nu c^2\left(\frac{\partial w_s}{\partial y}\right)^2\right)\right]\frac{\partial^2 w_s}{\partial x^2}$$
$$+12c^2\alpha_1\left[c\frac{\partial v_s}{\partial y} + \nu\frac{\partial u_s}{\partial x} + \frac{1}{2}\left(c^2\left(\frac{\partial w_s}{\partial y}\right)^2 + \nu\left(\frac{\partial v}{\partial x}\right)^2\right)\right]\frac{\partial^2 w_s}{\partial y^2}$$
$$+12c(1-\nu)\alpha_1\left[c\frac{\partial u}{\partial y} + \frac{\partial v}{\partial x} + c\frac{\partial w_s}{\partial x}\frac{\partial w_s}{\partial y}\right]\frac{\partial^2 w_s}{\partial x \partial y} = -\alpha_2\frac{(V_p)^2}{(1-w_s)^2} \tag{18}$$

In order to solve the above nonlinear equations, the Galerkin procedure was implemented. For this purpose, the solution of Eqs. (16) ~ (18) sought to be in the form of:

$$u_{m,n}(x, y) = C_{1m,n}Sin(2m\pi x)Sin\left((2n-1)\pi y\right)$$
$$u_{m,n}(x, y) = C_{2m,n}Sin\left((2m-1)\pi x\right)Sin(2n\pi y)$$
$$w_{m,n}(x, y) = C_{3m,n}Sin\left((2m-1)\pi x\right)Sin\left((2n-1)\pi y\right) \tag{19}$$
$$m, n = 1, 2, \ldots$$

Multiplying both sides of Eq. (18) by $(1-w_s(x,y))^2$, substituting Eq. (19) into the resulting equation, and also Eqs. (16) and (17), and then, appling the Galerkin method the $C_{m,n}$ values and displacements of the microplate are obtained.

In order to find the number of modes that must be retained in discretization for a desired accuracy, a convergence study is necessary. Figure 4 shows maximum deflection of the microplate associated to various mode numbers considered in Galerkin approach. Parameter values, used in this analysis, are $a = 310\mu m$ and

https://doi.org/10.1017/jmech.2012.19 Published online by Cambridge University Press

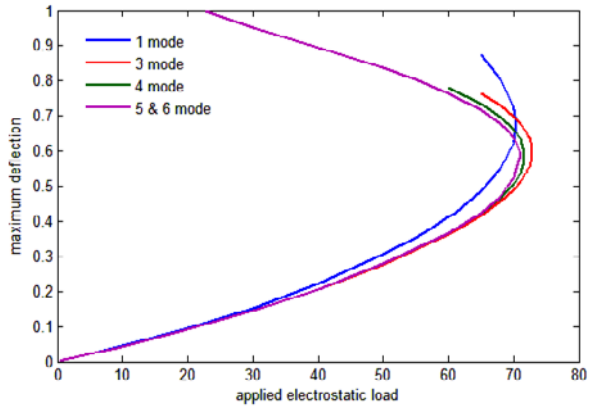


Fig. 4 Variations of maximum deflection of an immovable simply supported square microplate with the electrostatic load $\alpha_2 V_p^2$ for $\alpha_1 = 1$

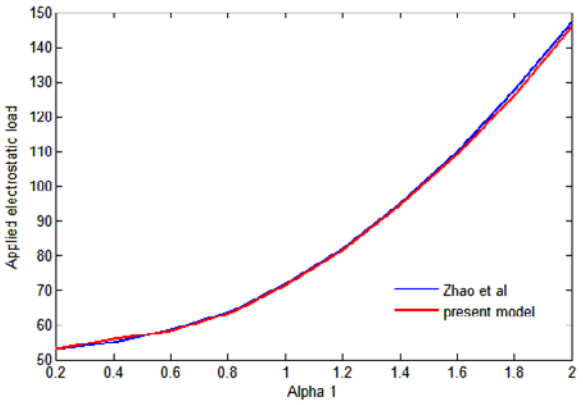


Fig. 5 Variations of electrostatic pull-in load with α_1 for simply supported square microplate

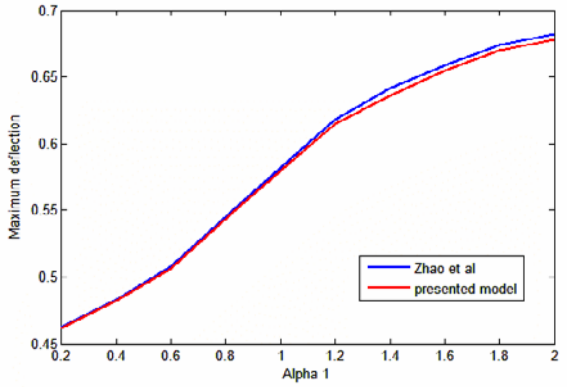


Fig. 6 Variations of maximum deflection with α_1 for simply supported square microplate

$\varepsilon_0 = 8.854 \times 10^{-12}$F/m. The microplate in this analysis is considered as a simply supported square SiO_2 microplate. As shown in Fig 4, at least five modes must be considered in the discretization approach.

In Figs. 5 and 6, Variations of $\alpha_2 V_p^2$ and $w_{\max}$ with respect to α_1 for the solution method used in this study, and the method proposed by Zhao *et al.* [22] are presented. In ref. [22] the linear mode shapes are obtained numerically using the hierarchical finite-element method. Then, the nonlinear partial-differential equations of the motion are reduced by the Galerkin method to a finite system of the nonlinearly coupled ordinary-differential equations.

As shown in Figs. 5 and 6, there is a good agreement between results. So, the presented model estimates the pull-in voltage with a good accuracy. As shown in these figures, the maximum difference between two methods is 0.3% for $\alpha_2 = 2$.

5. LINEAR EIGENVALUE PROBLEM

Removing nonlinear, damping and forcing terms from the governing equations of dynamic response of the microplate, the linear eigenvalue problem about the deflected position is derived as:

$$p_1\frac{\partial^2 u_d}{\partial x^2}+p_2\frac{\partial^2 v_d}{\partial x\partial y}+p_3\frac{\partial^2 u_d}{\partial y^2}+p_4\frac{\partial w_d}{\partial x}+p_5\frac{\partial w_d}{\partial y}+p_6\frac{\partial^2 w_d}{\partial x^2}+p_7\frac{\partial^2 w_d}{\partial y^2}+p_8\frac{\partial^2 w_d}{\partial x\partial y}+p_9\frac{\partial^2 u_d}{\partial t^2}=0 \tag{20}$$

$$q_1\frac{\partial^2 v_d}{\partial y^2}+q_2\frac{\partial^2 u_d}{\partial x\partial y}+q_3\frac{\partial^2 v_d}{\partial x^2}+q_4\frac{\partial w_d}{\partial x}+q_5\frac{\partial w_d}{\partial y}+q_6\frac{\partial^2 w_d}{\partial x^2}+q_7\frac{\partial^2 w_d}{\partial y^2}+q_8\frac{\partial^2 w_d}{\partial x\partial y}+q_9\frac{\partial^2 v_d}{\partial t^2}=0 \tag{21}$$

$$r_1\frac{\partial^4 w_d}{\partial x^4}+r_2\frac{\partial^4 w_d}{\partial x^2\partial y^2}+r_3\frac{\partial^4 w_d}{\partial y^4}+r_4\frac{\partial w_d}{\partial x}+r_5\frac{\partial w_d}{\partial y}+r_6\frac{\partial^2 w_d}{\partial x^2}+r_7\frac{\partial^2 w_d}{\partial y^2}+r_8\frac{\partial^2 w_d}{\partial x\partial y}+r_9\frac{\partial u_d}{\partial x}+r_{10}\frac{\partial u_d}{\partial y}+r_{11}\frac{\partial v_d}{\partial x}+r_{12}\frac{\partial v_d}{\partial y}+r_{13}\frac{\partial^2 w_d}{\partial t^2}+r_{14}\frac{\partial^2 u_d}{\partial t^2}+r_{15}\frac{\partial^2 v_d}{\partial t^2}=0 \tag{22}$$

in which:

$$p_1=1,\ p_2=\frac{1+\nu}{2},\ p_3=\frac{1-\nu}{2},\ p_4=\frac{1-\nu}{2}\frac{\partial^2 w_s}{\partial y^2}+\frac{\partial^2 w_s}{\partial x^2},$$
$$p_5=\frac{1+\nu}{2}\frac{\partial^2 w_s}{\partial x\partial y},\ p_6=\frac{\partial w_s}{\partial x},\ p_7=\frac{1-\nu}{2}\frac{\partial w_s}{\partial x},$$
$$p_8=\frac{1+\nu}{2}\frac{\partial w_s}{\partial y},\ p_9=\frac{-h^2}{12a^2}$$

$$q_1=1,\ q_2=\frac{1+\nu}{2},\ q_3=\frac{1-\nu}{2},\ q_4=\frac{1+\nu}{2}\frac{\partial^2 w_s}{\partial x\partial y},$$
$$q_5=\frac{1-\nu}{2}\frac{\partial^2 w_s}{\partial x^2}+\frac{\partial^2 w_s}{\partial y^2},\ q_6=\frac{1-\nu}{2}\frac{\partial w_s}{\partial y},\ q_7=\frac{\partial w_s}{\partial y},$$
$$q_8=\frac{1+\nu}{2}\frac{\partial w_s}{\partial x},\ q_9=\frac{-h^2}{12a^2}$$

https://doi.org/10.1017/jmech.2012.19 Published online by Cambridge University Press

$$r_1 = r_3 = 1, r_2 = 2,\ r_4 = -12\alpha_1 \frac{\partial w_s}{\partial x}\left(\frac{\partial^2 w_s}{\partial x^2} + \nu \frac{\partial^2 w_s}{\partial y^2}\right) - 12\alpha_1(1-\nu)\frac{\partial w_s}{\partial y}\frac{\partial^2 w_s}{\partial x \partial y},$$

$$r_5 = -12\alpha_1 \frac{\partial w_s}{\partial y}\left(\frac{\partial^2 w_s}{\partial y^2} + \nu \frac{\partial^2 w_s}{\partial x^2}\right) - 12\alpha_1(1-\nu)\frac{\partial w_s}{\partial x}\frac{\partial^2 w_s}{\partial x \partial y}$$

$$r_6 = -12\alpha_1 \frac{\partial u_s}{\partial x} - 12\alpha_1 \nu \frac{\partial v_s}{\partial y} - 6\alpha_1\left(\left(\frac{\partial w_s}{\partial x}\right)^2 + \nu\left(\frac{\partial w_s}{\partial y}\right)^2\right) - 12\frac{a^2}{h^2}N_1$$

$$r_7 = -12\alpha_1 \frac{\partial v_s}{\partial y} - 12\alpha_1 \nu \frac{\partial u_s}{\partial x} - 6\alpha_1\left(\left(\frac{\partial w_s}{\partial y}\right)^2 + \nu\left(\frac{\partial w_s}{\partial x}\right)^2\right) - 12\frac{a^2}{h^2}N_2 \tag{23}$$

$$r_8 = -12\alpha_1(1-\nu)\left(\frac{\partial u_s}{\partial y} + \frac{\partial v_s}{\partial x} + 2\frac{a^2}{h^2}N_{12} + \frac{\partial w_s}{\partial x}\frac{\partial w_s}{\partial y}\right)$$

$$r_9 = -12\alpha_1\left(\frac{\partial^2 w_s}{\partial x^2} + \nu \frac{\partial^2 w_s}{\partial y^2}\right),\ r_{1'0} = r_{11} = -12\alpha_1(1-\nu)\frac{\partial^2 w_s}{\partial x \partial y},\ r_{12} = -12\alpha_1\left(\frac{\partial^2 w_s}{\partial y^2} + \nu \frac{\partial^2 w_s}{\partial x^2}\right)$$

$$r_{13} = 1 + \frac{2\alpha_2 V_s^{\,2}}{(-1+w_s)^3},\ r_{14} = \alpha_1 \frac{h^2}{a^2}\frac{\partial w_s}{\partial x},\ r_{15} = \alpha_1 \frac{h^2}{a^2}\frac{\partial w_s}{\partial y}$$

In order to solve Eqs. (20) ~ (22) let

$$\begin{aligned} u_d(x, y, t) &= U(x, y)\, e^{i\omega_{m,n}t} \\ v_d(x, y, t) &= V(x, y)\, e^{i\omega_{m,n}t} \\ w_d(x, y, t) &= W(x, y)\, e^{i\omega_{m,n}t} \end{aligned} \tag{24}$$

where

$$\begin{aligned} &U(x,y) = B_{1m,n}\, \Phi_{u\,m,n}(x,y),\ V(x,y) = B_{2m,n}\, \Phi_{v\,m,n}(x,y), \\ &W(x,y) = B_{3m,n}\, \Phi_{w\,m,n}(x,y) \end{aligned} \tag{25}$$

in which Φ is the linear undameped mode shape of undeflected microplate.

Substituting Eqs (24) and (25) and the solution of Eqs. (16) ~ (18) into Eqs. (20) ~ (22) and applying Galerkin method, natural frequencies and mode shapes of the microplate about the deflected position are derived.

6. VISCOELASTIC DAMPING QUALITY FACTOR

Substituting Eq. (24) into equations of dynamic response of the microplate and keeping the linear terms, the differential equations of system have been obtained. The difference between these equations and Eqs. (20) ~ (22) is the presence of the damping and forcing terms in these equations. Here, the quality factor of structural damping is obtained by using strained parameters perturbation technique. For this purpose, it is assumed that:

$$\begin{aligned} U(x, y) &= U_0(x, y) + \varepsilon U_1(x, y) \\ V(x, y) &= V_0(x, y) + \varepsilon V_1(x, y) \\ W(x, y) &= W_0(x, y) + \varepsilon W_1(x, y) \\ \omega_{m,n} &= \omega^0_{m,n} + \varepsilon\, \omega^1_{m,n} \end{aligned} \tag{26}$$

where ε is a small bookkeeping parameter. Considering Eq. (5), it is necessary to recall that $\eta^* = \eta/\tau$. So, one can rewrite $\eta^* = C/E\tau$. Hence, $\eta^*\omega^0_{m,n}$ is equal to $C\omega^0_{m,n}/E\tau$, where parameter $C\omega^0_{m,n}/\tau = C\omega_t$ is known as the "loss". Considering that *loss* << *E*, and substituting Eq. (26) into differential equations of system, and equating the terms with like powers of ε, one can obtain:

$\varepsilon^{(0)}$

$$\begin{aligned} &L_1(U_0, V_0, W_0) = \\ &p_1\frac{\partial^2 U_0}{\partial x^2} + p_2\frac{\partial^2 V_0}{\partial x \partial y} + p_3\frac{\partial^2 U_0}{\partial y^2} + p_4\frac{\partial W_0}{\partial x} + p_5\frac{\partial W_0}{\partial y} \\ &+ p_6\frac{\partial^2 W_0}{\partial x^2} + p_7\frac{\partial^2 W_0}{\partial y^2} + p_8\frac{\partial^2 W_0}{\partial x \partial y} + p_9' U_0 = 0 \end{aligned} \tag{27}$$

$$\begin{aligned} &L_2(U_0, V_0, W_0) = \\ &q_1\frac{\partial^2 V_0}{\partial y^2} + q_2\frac{\partial^2 U_0}{\partial x \partial y} + q_3\frac{\partial^2 V_0}{\partial x^2} + q_4\frac{\partial W_0}{\partial x} + q_5\frac{\partial W_0}{\partial y} \\ &+ q_6\frac{\partial^2 W_0}{\partial x^2} + q_7\frac{\partial^2 W_0}{\partial y^2} + q_8\frac{\partial^2 W_0}{\partial x \partial y} + q_9' V_0 = 0 \end{aligned} \tag{28}$$

$$\begin{aligned} &L_3(U_0, V_0, W_0) = \\ &r_1\frac{\partial^4 W_0}{\partial x^4} + r_2\frac{\partial^4 W_0}{\partial x^2 \partial y^2} + r_3\frac{\partial^4 W_0}{\partial y^4} + r_4\frac{\partial W_0}{\partial x} + r_5\frac{\partial W_0}{\partial y} \\ &+ r_6\frac{\partial^2 W_0}{\partial x^2} + r_7\frac{\partial^2 W_0}{\partial y^2} + r_8\frac{\partial^2 W_0}{\partial x \partial y} + r_9\frac{\partial U_0}{\partial x} \\ &+ r_{10}\frac{\partial U_0}{\partial y} + r_{11}\frac{\partial V_0}{\partial x} + r_{12}\frac{\partial V_0}{\partial y} + r_{13}' W_0 + r_{14}' U_0 + r_{15}' V_0 = 0 \end{aligned} \tag{29}$$

https://doi.org/10.1017/jmech.2012.19 Published online by Cambridge University Press

$\varepsilon^{(1)}$

$$L_1(U_1, V_1, W_1) = -I\eta\omega_0\left\{p_1\frac{\partial^2 U_0}{\partial x^2}+p_2\frac{\partial^2 V_0}{\partial x\partial y}+p_3\frac{\partial^2 U_0}{\partial y^2}+p_4\frac{\partial W_0}{\partial x}+p_5\frac{\partial W_0}{\partial y}+p_6\frac{\partial^2 W_0}{\partial x^2}+p_7\frac{\partial^2 W_0}{\partial y^2}+p_8\frac{\partial^2 W_0}{\partial x\partial y}\right\}-\frac{h^2}{6a^2}\omega_0\,\omega_1 U_0 = f_1 \tag{30}$$

$$L_2(U_1, V_1, W_1) = -I\eta\omega_0\left\{q_1\frac{\partial^2 V_0}{\partial y^2}+q_2\frac{\partial^2 U_0}{\partial x\partial y}+q_3\frac{\partial^2 V_0}{\partial x^2}+q_4\frac{\partial W_0}{\partial x}+q_5\frac{\partial W_0}{\partial y}+q_6\frac{\partial^2 W_0}{\partial x^2}+q_7\frac{\partial^2 W_0}{\partial y^2}+q_8\frac{\partial^2 W_0}{\partial x\partial y}\right\}-\frac{h^2}{6a^2}\omega_0\,\omega_1 V_0 = f_2 \tag{31}$$

$$L_3(U_1, V_1, W_1) = I\eta\omega_0\left\{r_1\frac{\partial^4 W_0}{\partial x^4}+r_2\frac{\partial^4 W_0}{\partial x^2\partial y^2}+r_3\frac{\partial^4 W_0}{\partial y^4}+r_4\frac{\partial W_0}{\partial x}+r_5\frac{\partial W_0}{\partial y}+r_9\frac{\partial U_0}{\partial x}+r_{10}\frac{\partial U_0}{\partial y}+r_{11}\frac{\partial V_0}{\partial x}+r_{12}\frac{\partial V_0}{\partial y}\right\}+\left\{2\alpha_1\frac{h^2}{a^2}\left(\frac{\partial w_s}{\partial x}U_0+\frac{\partial w_s}{\partial y}V_0\right)-2W_0\right\}\omega_0\,\omega_1 = f_3 \tag{32}$$

Equations (27) ~ (29) are the same as Eqs. (20) ~ (22), but:

$$p_9' = \frac{h^2\,\omega_0^2}{12\,a^2},\ q_9' = \frac{h^2\,\omega_0^2}{12\,a^2},\ r_{13}' = -{\omega_0}^2+\frac{2\alpha_2\,{V_s}^2}{(-1+w_s)^3},\ r_{14}' = \alpha_1\frac{h^2\omega_0^2}{a^2}\frac{\partial w_s}{\partial x},\ r_{15}' = \alpha_1\frac{h^2\omega_0^2}{a^2}\frac{\partial w_s}{\partial y} \tag{33}$$

In fact, Eqs. (27) ~ (29) are the differential equations of the system without damping effect.

Since the homogeneous system of equations given by Eqs. (30) ~ (32) has a nontrivial solution, the inhomogeneous system has a solution only if a solvability condition is satisfied [23]. To determine this solvability condition, one must multiply both sides of Eqs. (30) ~ (32) by U_1^*, V_1^* and W_1^*, the adjoint solutions of U_1, V_1, W_1, and integrate by parts to transfer derivatives into adjoint solutions. So one can obtain:

$$\iint\left\{U_1L_1^*(U_1^*,V_1^*,W_1^*)+V_1L_2^*(U_1^*,V_1^*,W_1^*)+W_1L_3^*(U_1^*,V_1^*,W_1^*)\right\}dx\,dy = \iint\{U_1^*\,f_1+V_1^*\,f_2+W_1^*\,f_3\}\,dx\,dy \tag{34}$$

with U_1^*, V_1^* and W_1^* satisfying the adjoint equations of homogeneous system, the solvability condition is reduced to:

$$\iint\{U_1^*\,f_1+V_1^*\,f_2+W_1^*\,f_3\}\,dx\,dy = 0 \tag{35}$$

Upon substituting of f_1, f_2 and f_3 into the above equation, the resulting equation will be obtained in term of ω_0, ω_1 and η:

$$i\eta\iint H_1(x,y)\,dx\,dy+\omega_1\iint H_2(x,y)\,dx\,dy = 0 \tag{36}$$

where

$$H_2(x,y) = -U_1^*\frac{h^2}{6a^2}\omega_0\,U_0-V_1^*\frac{h^2}{6a^2}\omega_0\,V_0+W_1^*\left\{2\alpha_1\frac{h^2}{a^2}\left(\frac{\partial w_s}{\partial x}U_0+\frac{\partial w_s}{\partial y}V_0\right)-2W_0\right\}\omega_0$$

$$H_1(x,y) = \frac{1}{I\eta}\left\{U_1^*f_1+V_1^*f_2+W_1^*f_3-H_2(x,y)\right\} \tag{37}$$

and so:

$$\omega_1 = -\frac{i\eta\iint H_1(x,y)\,dx\,dy}{\iint H_2(x,y)\,dx\,dy} \tag{38}$$

So, the damping quality factor of the viscoelastic microplate will be obtained as:

$$Q_{visco}^{-1} = \frac{2\,\mathrm{Im}(\omega_1)}{\omega_0+\mathrm{Re}(\omega_1)} = \frac{loss\times H}{E} \tag{39}$$

7. RESULTS AND DISCUSSIONS

As shown in Fig. 3, Young's modulus of a SWNT/PMMA nanocomposite linearly is increased when the volume fraction of SWNT is increased. It means that the microplate is being stiffer when the reinforcement is increased. This fact directly affects the pull-in instability of the microplate. As the volume fraction increases, the stiffness of the microplate increases, and simultaneously, the density of the microplate also increase. The rate of the increasing of these parameters and the influence of them on the deflection and frequency of the microplate are important matters that should be investigated.

Figure 7 shows the variations of the pull-in voltage with respect to CNT volume percentage of nanocomposite. The pull-in voltage is increased linearly when the CNT percentage is increased, and for $V_f \approx 32.2\%$, the pull-in voltage of SWNT/PMMA composite and SiO_2 plate become similar.

The natural frequency of vibration and stiffness of an actuating structure such as a microswitch are measures of the response time and the force required for a specified deformation. For a specific deformation, the response time is decreased as the natural frequency is increased, and the required force is decreased as the stiffness is decreased. Simultaneous decreasing of the response time and the required force would be a desired characteristic in such devices.

The natural frequency of the microplates when the electrostatic voltage is increased for $\alpha_1 = 1$ has been presented in Fig. 8. As shown in this figure, for volume fractions of SWNT greater than 15%, the natural frequency of nanocomposite microplates are higher than SiO_2 microplate. Also Fig. 9 compares transverse

https://doi.org/10.1017/jmech.2012.19 Published online by Cambridge University Press

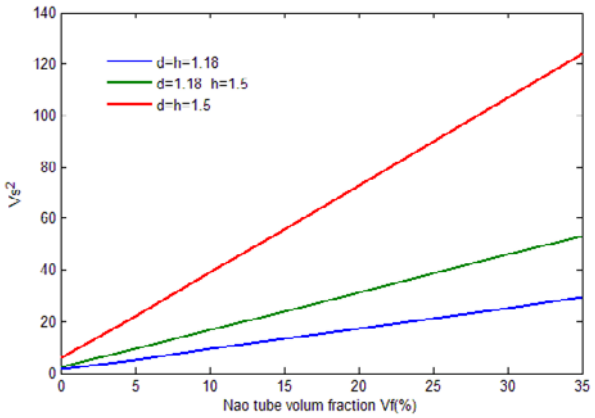


Fig. 7 Variations of pull in voltage with nano tube volume fraction

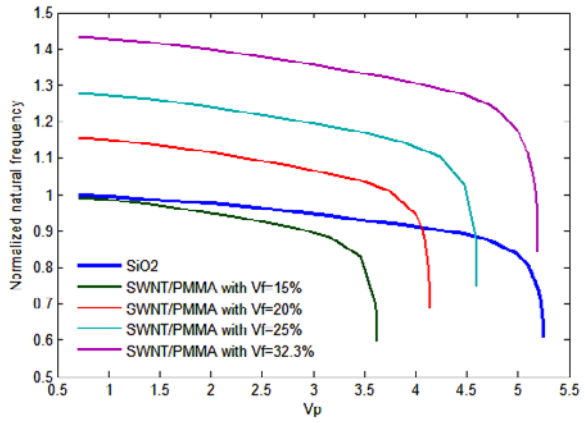


Fig. 8 Variations of natural frequency of the microplate with applied electrostatic voltage

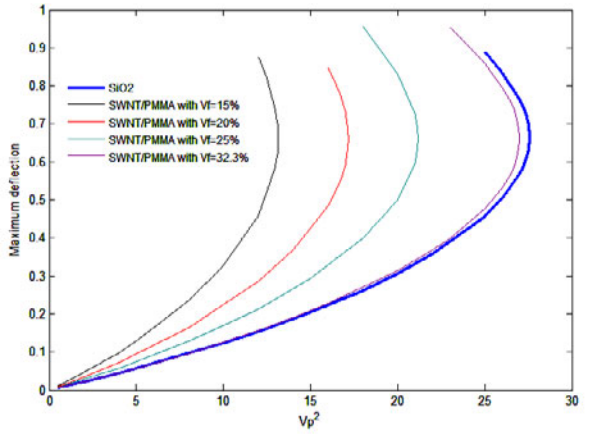


Fig. 9 Maximum deflection of microplates related to applied electrostatic voltage for different volume fraction of nanotube

deflection of SWNT/PMMA nanocomposite microplates with the one of SiO_2 microplate. As shown in this figure, for a given voltage, the displacement of the microplate is increased as the SWNT volume fraction is decreased. Considering Fig. 8, although the natural frequency of 15% SWNT/PMMA microplate, for electrostatic voltages lower than pull-in voltage, is nearly equal to the one of SiO_2 microplate, its deflection is higher than the deflection of SiO_2 microplate (Fig. 9). So, the pull-in instability of the nanocomposite microplate would happen sooner. Furthermore, the maximum deflection of the microplate, for applied voltages beyond pull in voltage, for a 32.3% SWNT/PMMA nanocomposite microplate is equal to the one of SiO_2 microplate, and its natural frequency is about 1.4 times of SiO_2 one that results in a 30% decreasing of the response time. This is a very useful and favorable characteristic in microswithes.

Figure 10 shows the variation of H with respect to applied electrostatic voltage. As shown in this figure, this parameter is increased as applied voltage is increased, and goes to infinity for the pull-in voltage. There is an ω_0 term in denominator of H. As applied voltage is increased, the natural frequency is decreased and goes to zero for the pull-in voltage, and consequently, the values of H goes to infinity for pull-in voltage. Also when applied voltage goes to zero the values of H would be equal to 1, and so, when $V_p = 0$, for every values of other parameters, the values of the quality factor becomes equal to $Q_{visco}^{-1} = loss / E$.

The variations of H with respect to volume fraction of SWNT have been shown in Fig. 11. As shown in this figure, the value of H is decreased as volume fraction is increased. It means that for higher values of SWNT volume fraction, the quality factor Q_{visco}^{-1} is decreased. The value of Q_{visco}^{-1}, simultaneously, depends on the value of H and the *loss*. As mentioned in the literatures, the values of η, for ceramics such as SiO_2 is in the range of $10^{-4} \sim 10^{-5}$ [24], and for example, for 10% volume fraction carbon nanotube reinforced composite is in the range of $10^{-1} \sim 10^{-2}$ [25]. So, the quality factor Q_{visco}^{-1} of SWNT/PMMA is widely different from SiO_2 that means the damping of such nanocomposites is much greater than SiO_2. This characteristic highly affects the implementation of viscoelastic nanocomposites. In the other words, using viscoelastic nanocomposite materials for a resonator is not recommended unless a material selection and an optimization procedure on the volume fraction of its components perform. The optimization is necessary to avoid the pull-in instability of the microplate and to adjust the damping of microplate material.

In general, in comparison to other materials, nanocomposites are in a great deal of interest due to the broad opportunity of setting parameters to achieve more favorite behavior. In spite of these advantages, one needs to account for high damping characteristics of a SWNT/PMMA microplate as a viscoelastic material and to study the damping influence when an AC voltage is applied

8. CONCLUSIONS

In this paper, the governing equations of motion of a viscoelastic material about its static deflection have

https://doi.org/10.1017/jmech.2012.19 Published online by Cambridge University Press

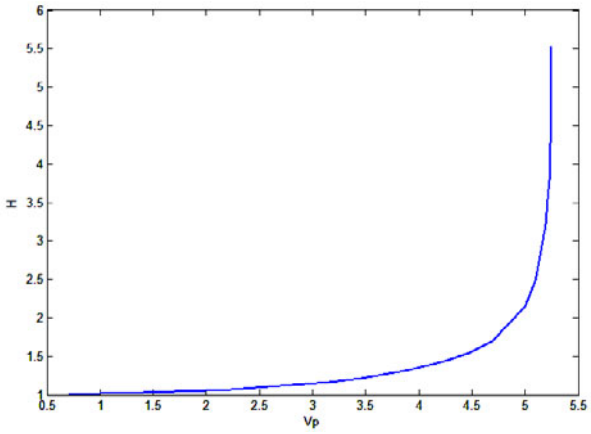


Fig. 10 Variation of H to electrostatic voltage V_p

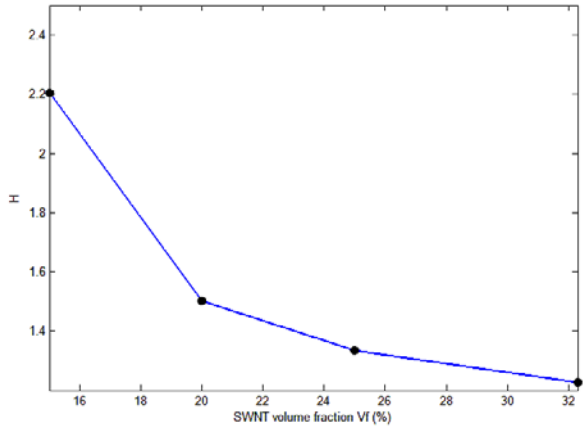


Fig. 11 Variation of H to SWNT volume fraction

been obtained and solved by the Galerkin method. By using the Eshelby–Mori–Tanaka method, material characteristics of SWNT/PMMA composite have been extracted and the natural frequency and deflection of a nanocomposite microplate have been studied. The variations of the pull-in voltage with respect to volume fractions of SWNT have been studied and it has been demonstrated that it increases linearly as V_f increases. It has been shown that the nanocomposite microplate can be operates with the same displacement of the SiO_2 microplate together with higher frequency than the one of SiO_2. This characteristic is highly favorable for micro switches, micro resonators, micro dispensers, *etc*. But, the viscoelastic quality factor Q_{visco}^{-1} of nanocomposite microplate is much higher than the SiO_2 one that limits the implementation of PMMA nanocomposite for microresonators and reduces its application for microswithes.

REFERENCES

1. Zengerle, R., Richter, A. and Sandmaier, H., "A Micro Membrane Pump with Electrostatic Actuation," *Proceedings of Micro Electro Mechanical Systems Conference,* Germany (1992).
2. Zhang, X. M., Chau, F. S., Quan, C., Lam, Y. L. and Liu, A. Q., "A Study of the Static Characteristics of a Torsional Micromirror," *Sensors Actuators A*, **90**, pp. 73–81 (2001).
3. Hsu, P. C., Mastrangelo, C. H. and Wise, K. D., "A High Sensitivity Polysilicon Diaphragm Condenser Microphone," *Proceedings of MEMS Conference Heidelberg*, Germany, (1998).
4. Scheeper, P. R., van der Donk, A. G. H. and Bergveld, P., "A Review of Silicon Microphones," *Sensors Actuators A*, **44**, pp. 1–11 (1999).
5. Tilmans, H. A. and Legtenberg, R., "Electrostatically Driven Vacuum-Encapsulated Polysilicon Resonators: Part II. Theory and Performance," *Sensors Actuators A*, **45**, pp. 67–84 (1994).
6. Francais, O. and Dufour, I., "Normalized Abacus for the Global Behavior of Diaphragms: Pneumatic, Electrostatic, Piezoelectric or Electromagnetic Actuation," *Journal of Modelling and Simulation of Microsystems*, **1**, pp. 149–160 (1999).
7. Ng, T. Y., Jiang, T. Y., Li, H., Lam, K. Y. and Reddy, J. N., "A Coupled Field Study on the Non-Linear Dynamic Characteristics of an Electrostatic Micropump," *Journal of Sound and Vibration*, **273**, pp. 989–1006 (2004).
8. Porfiri, M., "Vibrations of Parallel Arrays of Electrostatically Actuated Microplates," *Journal of Sound and Vibration*, **315**, pp. 1071–1085 (2008).
9. Ashrafi, B., Hubert, P. and Vengallatore, S., "Carbon Nanotube-Reinforced Composites as Structural Materials for Microactuators in Microelectromechanical Systems," *Nanotechnology*, **17**, pp. 4895–4903 (2006).
10. Shen, G. R., Cheng, Y. T. and Tsai, L. N., "Synthesis and Characterization of Ni–P–CNT Nanocomposite Film for MEMS Applications," *IEEE Transactions on Nanotechnology*, **4**, pp. 539–547 (2005).
11. Tsai, L. N., Cheng, Y. T., Hsu, W. and Fang, W., "Ni–Carbon Nanotubes Nanocomposite for Robust Microelectromechanical Systems Fabrication," *Journal of Vacuum Science & Technology B: Microelectronics and Nanometer Structures*, **24**, pp. 205–210 (2006).
12. Fang, W., Chu, H. Y., Hsu, W. K., Cheng, T. W. and Tai, N. H., "Polymer-Reinforced Aligned Multiwalled Carbon Nanotube Composites for Microelectromechanical Systems Applications," *Advances in Materials*, **17**, pp. 2987–2992 (2005).
13. Coleman, J. N., Khan, U., Blau, W. J. and Gun'ko, Y. K., "Small But Strong: A Review of the Mechanical Properties of Carbon-Nanotube-Polymer Composites," *Carbon*, **44**, pp. 1624–1652 (2006).
14. Coleman, J. N., Khan, U. and Gun'ko, Y. K., "Mechanical Reinforcement of Polymers Using Carbon Nanotubes," *Advances in Materials*, **18**, pp. 689–706 (2006).
15. Thostenson, E. T., Li, C. and Chou, T. W., "Nanocomposites in Context," *Composites Science and Technology*, **65**, pp. 491–516 (2005).

https://doi.org/10.1017/jmech.2012.19 Published online by Cambridge University Press

16. Fu, Y. M. and Zhang, J., "Nonlinear Static and Dynamic Responses of an Electrically Actuated Viscoelastic Microbeam," *Acta Mechanica Sinica*, **25**, pp. 211–218 (2009).
17. Fu, Y. M., Zhang, J. and Bi, R. G., "Analysis of the Nonlinear Dynamic Stability for an Electrically Actuated Viscoelastic Microbeam," *Microsystem Technologies*, **15**, pp. 763–769 (2009).
18. Fu, Y. and Zhang, J., "Active Control of the Nonlinear Static and Dynamic Responses for Piezoelectric Viscoelastic Microplates," *Smart Materials and Structures*, **18**, 095037 (9pp) (2009).
19. Zamanian, M., Khadem, S. E. and Mahmoodi, S. N., "Nonlinear Response of a Resonant Viscoelastic Microbeam Under an Electrical Actuation," *Structural Engineering and Mechanics*, **35**, pp. 387–407 (2010).
20. Iijima, S., "Helical Microtubules of Graphitic Carbon," *Nature*, **354**, pp. 56–58 (1991).
21. Chen, C. H. and Cheng, C. H., "Effective Elastic Moduli of Misoriented Short-Fiber Composites," *International Journal of Solids and Structures*, **33**, pp. 2519–2539 (1996).
22. Zhao, X. P., Abdel-Rahman, E. M. and Nayfeh, A. H., "A Reduced-Order Model for Electrically Actuated Microplates," *Journal of Micromechanics and Microengineering*, **14**, pp. 900–906 (2004).
23. Nayfeh, A. H., *An Introduction to Perturbation Techniques*, Wiley, New York (1981).
24. Cebon, D. and Ashby, M. F., "Material Selection for Precision Instruments," *Measurement Science and Technology*, **5**, pp. 296–306 (1994).
25. Kireitseu, M. V., "Preliminary Results on Rheological and Damping Properties of Nanoparticle-Reinforced Materials," *Annual Transactions of the Nordic Rheology Society*, **14** (2006).

(Manuscript received October 20, 2010,
accepted for publication August 15, 2011.)

https://doi.org/10.1017/jmech.2012.19 Published online by Cambridge University Press